Estimating the Parameters of Sinusoids and Decaying Sinusoids in Noise

Elias Aboutanios

Picture a low earth orbit satellite hurtling around the earth in an 800 km orbit. At this altitude, the satellite travels about 7.5 km every second, and any signals between it and an earth terminal experience significant Doppler shifts. These frequency offsets must be estimated and removed at the earth terminal to enable successful communications with the satellite. As in this example, the estimation of the parameters of a sinusoid plays a fundamental role in a variety of applications ranging from seismology to radar and biological signals. Therefore, this problem has received, and continues to receive, significant attention in the literature. In power delivery systems, the estimation of the supply frequency is required for the monitoring of the system quality and the detection of faults [1], [2]. In nuclear magnetic resonance spectroscopy (NMRS), on the other hand, the signal is modelled as a sum of decaying complex exponentials whose frequencies and decay factors must be estimated [3].

The advent of computing and the subsequent introduction of the fast Fourier transform (FFT) algorithm revolutionized the digital processing of signals. The FFT algorithm provides a highly efficient implementation of the discrete Fourier transform (DFT) on a regularly sampled grid. This efficiency and suitability for fast implementations on digital signal processors have made the FFT a very successful and widely used algorithm. It is no surprise that it has come to form the basis for a significant number of parameter estimators.

In this article, we examine the problem of estimating the frequency and decay factor of sinusoids in noise. In particular, we focus on frequency-domain (i.e. DFT-based) estimators that take advantage of the efficient FFT algorithm. We start by presenting the general signal model. We then discuss the estimation of the frequency of an un-damped sinusoid before moving onto the estimation of the frequency and decay factor of a damped complex exponential. Finally, we conclude with some brief remarks regarding the multi-component and real sinusoid cases.

The Signal Model

Suppose that we have a block of N samples of a complex exponential in additive noise,

$$\begin{aligned} x[k] &= s[k] + w[k] \\ &= Ae^{(-\eta + j2\pi f)k} + w[k], \quad \text{for } k = 0 \ldots N-1, \end{aligned} \tag{1}$$

where A is the complex amplitude (that is $A = |A| e^{j\varphi}$ and φ is the initial phase), f the signal frequency, and η the decay factor. We assume that f is normalised to the sampling rate f_s, which guaranties that $f \in [-0.5, 0.5]$. The terms, $w[k]$, are generally taken to be additive white Gaussian Noise (AWGN) with zero-mean and independent and identically distributed real and imaginary parts having variance $\sigma^2/2$. The signal to noise ratio (SNR), which we denote by ρ, is given by the power of the signal over that of the noise $\rho = |A|^2/\sigma^2$. Although the AWGN noise model is adopted here, the estimators we discuss in what follows work under more general noise conditions, see [4], and have been applied in other noise environments such as mixed Gaussian, as well as impulsive noise [5].

The Frequency of an Un-Damped Complex Exponential

The decay factor has a fundamental impact on the SNR and consequently on the achievable estimation performance. Therefore, in this section, we focus on the estimation of the frequency of an un-damped exponential. The decaying case will then be addressed separately later on.

The Maximum Likelihood Estimator of the Frequency

The maximum likelihood estimate (MLE) of a parameter is the value that gives the highest probability (the *likelihood*) of observing the given set of measurements. Given a block of N samples, the MLE of the frequency is the value that maximizes the likelihood of actually obtaining these N samples when the measurement is performed. Rife and Boorstyn in [6] showed that the MLE of the frequency is given by the maximiser of the periodogram,

$$\hat{f}_{ML} = \arg\max_{\lambda} I(\lambda), \tag{2}$$

where the periodogram is defined as $I(\lambda) = |X(\lambda)|^2$ for

$$X(\lambda) = \sum_{k=0}^{N-1} x[k] e^{-j2\pi k\lambda}. \tag{3}$$

Fig. 1 shows a plot of $I(\lambda)$ for a noiseless signal with N = 32 and f = 0.145. Observe that it exhibits a maximum at the

1094-6969/11/$25.00©2011IEEE

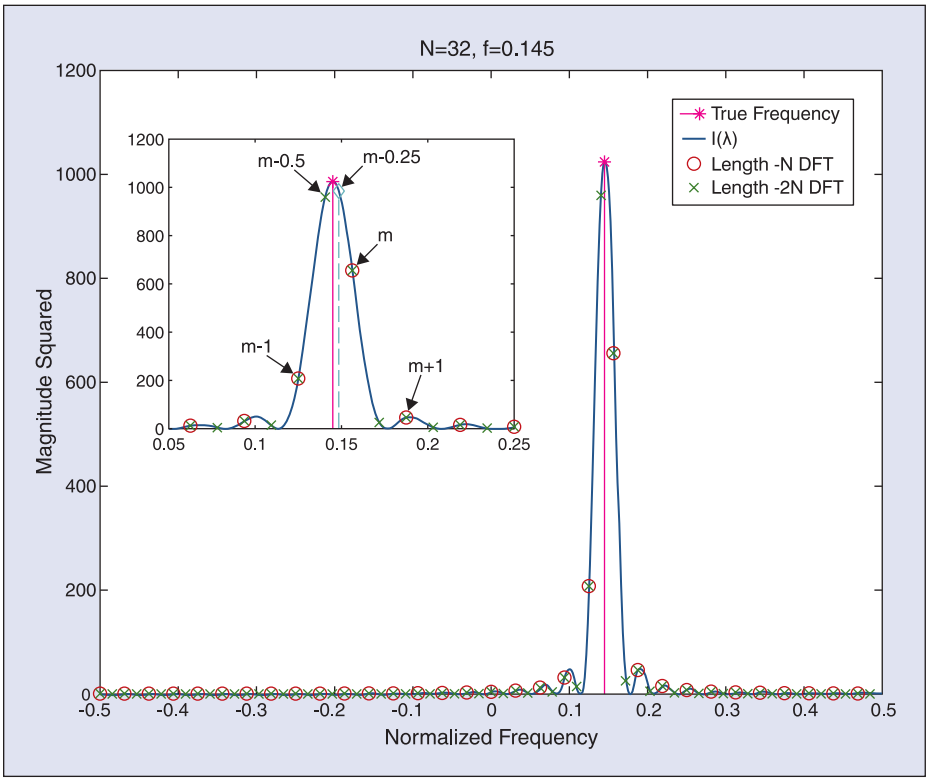

Fig. 1. A plot of the periodogram function $I(\lambda)$ and periodograms calculated from DFTs of lengths N and $2N$. The position of the true signal frequency is marked. The inset depicts a binary search for the peak.

true signal frequency. In fact, looking at (3) we see that the MLE effectively produces the frequency that maximizes the projection of the observed samples on to the template $e^{-j2\pi k\lambda}$. The MLE is known to be optimal under Gaussian noise conditions as it is unbiased and achieves the lowest variance of any possible estimator.

The Performance Bound and Threshold Effect

When parameters are estimated from noisy observations, it is important to have an indication of the best attainable estimation performance. The Cramer-Rao lower bound (CRLB) provides such a benchmark, setting a lower bound on the achievable estimation variance. Additionally, nonlinear estimators are known to be plagued by threshold effects. As the SNR drops, a point is reached below which the estimator breaks down with the variance increasing rapidly. We refer to this point as the threshold SNR. An estimator with a lower threshold is said to be more robust at low SNRs.

The Cramer Rao Lower Bound

The CRLB, $\tilde{\sigma}_f^2$, of the frequency of a complex exponential in noise was derived in [6]. For any estimator of frequency, the estimation variance $\sigma^2{}_f$ must satisfy the inequality $\sigma_f^2 \geq \tilde{\sigma}_f^2$ where

$$\tilde{\sigma}_f^2 = \frac{6f_s^2}{(2\pi)^2 \rho N\left(N^2-1\right)}. \qquad (4)$$

The MLE is an un-biased estimator that achieves the CRLB and is therefore referred to as an efficient estimator. Notice that as N increases, the CRLB decreases as N^{-3} which we write as $O(N^{-3})$. Furthermore, the logarithm of the CRLB varies linearly with respect to the SNR expressed in decibels.

The SNR Threshold Effect

The MLE aims to locate the peak of the main lobe in Fig. 1, which can be achieved reliably at high SNR. For low enough SNRs, however, a noise term may happen to be larger than the signal component. This is called an outlier, and its probability of occurrence, q_N, is given in [6] by

$$q_N = 1 - \int_0^{\infty} \left[1 - e^{-N\frac{r^2}{2\sigma^2}}\right]^{N-1} \frac{Nr}{\sigma^2} e^{-N\frac{r^2+|A|^2}{2\sigma^2}} I_0\left(\frac{N|A|r}{\sigma^2}\right) dr. \qquad (5)$$

Here, $I_0(x)$ is the modified Bessel function of the first kind. Now as the SNR decreases, we reach a point where the rapidly increasing outlier probability produces a sharp increase in the estimation variance. This point is called the SNR threshold. Knowing the value of the threshold is essential to determine the useful SNR operating range of the algorithms.

The Optimal Estimation Variance

The CRLB and the outlier probability are now combined to give a lower bound on the estimation performance. When the maximum bin is correctly chosen, the estimation error is almost entirely confined to the main lobe and its variance is lower bounded by the CRLB. This occurs with a probability $1-q_N$. When an outlier occurs, on the other hand, any of the bins corresponding to frequencies in the range [–0.5, 0.5] are equally likely, and the estimation variance is effectively due to a uniform distribution over the estimation interval, giving it a value of $1/12$ (or in general $f_s^2/12$). Putting these two cases together [6], the total mean squared error becomes

$$\sigma_{TOT}^2 \approx q_N \frac{1}{12} + \left(1-q_N\right)\frac{6}{(2\pi)^2 \rho N\left(N^2-1\right)}. \qquad (6)$$

Fig. 2 shows a plot of σ_{TOT}^2 versus SNR for various values of N. The threshold is clearly visible and decreases with increasing N. Any SNR above the threshold can be considered as a "high SNR" since the estimation variance is bounded by

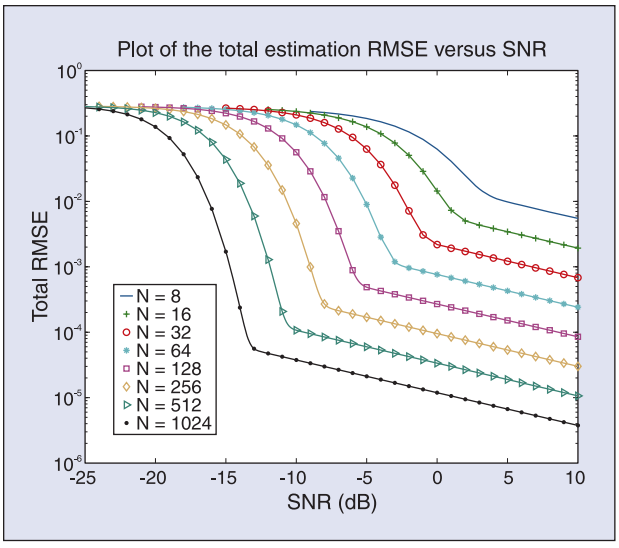

Fig. 2. Plots showing the total RMSE as a function of the signal to noise ratio.

the CRLB. A good estimator should have a threshold that is as near as possible to that of the MLE and an estimation variance above it that is as close as possible to the CRLB. That is, we desire estimators whose performance is as close to the relevant optimal curve in Fig. 2 as possible.

Practical Estimators

The ML estimator requires the maximization of the non-linear function $I(\lambda)$. This is a computationally difficult and intensive task that is hampered by the presence of local maxima and plagued by numerical problems [4]. However, $I(\lambda)$ can be efficiently evaluated (to within a scaling factor) on a regularly sampled grid using the DFT which we define here as

$$X\left[n\right]=\sum_{k=0}^{N-1}x[k]e^{-j2\pi k\frac{n}{N}},\ \text{for}\ n=0\ldots N-1. \tag{7}$$

Fig. 1 shows that the DFT-based periodogram samples sit on the curve for $I(\lambda)$. In other words, the DFT can be used to produce a sampled version of the periodogram which suggests that its maximum can be employed to estimate the frequency. We refer to this estimator as the maximum bin search (MBS). The major drawback of the MBS, however, is that its resolution is limited to $1/N$ which is a fixed resolution that is independent of the SNR and falls far short of the CRLB. Thus, as Fig. 3 shows, the MBS (represented by the curve corresponding to $L = 32$) is at best a coarse estimator at SNRs above the threshold, and techniques for improving the performance are clearly necessary. Such strategies are discussed next.

The Zero-Padded DFT

Given that the DFT samples the periodogram, a simple way to improve the resolution of the MBS is to increase the density of the samples on the frequency axis. This is easily achieved by padding the data with zeroes to some length $L \geq N$. For instance, the length-2N DFT in Fig. 1 produces a bin that is much closer to the true maximum. The resulting algorithm is called the zero-padded or ZP(L) estimator, and its resolution improves to $1/L$. Let $m = [Lf]$, where $[\bullet]$ indicates rounding $\bullet$ to the nearest integer. Then the signal frequency can be expressed as $f=\frac{m+\delta}{L}$, where $-0.5\leq\delta\leq0.5$ is the frequency residual. In the absence of noise, the ZP(L) algorithm returns the bin index m leaving the residual δ as the estimation error (or δ/L in Hz.) If no prior knowledge on the frequency is available, and noting that $|\delta|\leq0.5$, then δ is uniformly distributed over [–0.5, 0.5] and the estimation variance becomes

$$\hat{\sigma}_f^2=\frac{1}{12L^2}. \tag{8}$$

Fig. 3 illustrates the variance of the ZP(L) estimator for a number of values of L. Notice that even with $L = 1024$, the estimates are much poorer than the CRLB for any reasonable SNR above the threshold. Another observation is that the unpadded estimator has the worst threshold. This is easily explained by referring to Fig. 1 which shows that as δ moves toward ±0.5, as the true frequency deviates from the bin centre, the magnitude of the maximum bin decreases and so does its effective SNR. This is a direct consequence of the spectral leakage produced by the finite record length. As a result, the threshold of the un-padded estimator is about 2 dB worse than the theoretical curve.

A useful measure of the estimation performance is the ratio of the variance to the CRLB which gives the loss with respect to the optimum. For the ZP(L) algorithm, this is

$$R_{CRLB}^{ZP(L)}=\max\left\{1,\frac{(2\pi)^2\rho N\left(N^2-1\right)}{72L^2}\right\}, \tag{9}$$

where taking the maximum ensures that the ratio is lower-bounded by 1 as the variance is lower-bounded by the CRLB. Although increasing L allows us to decrease the variance, the performance is still independent of the SNR in contrast to the optimum which decreases as the SNR increases. In fact, as the

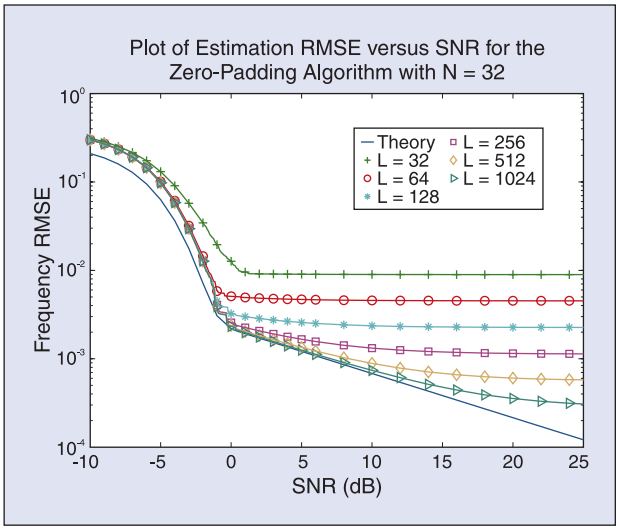

Fig.3. Plot of the performance of the zero-padding estimator as a function of signal to noise ratio.

SNR increases, the amount of zero padding required to match the CRLB quickly becomes computationally expensive. For example, for N = 32 and ρ = 0 dB, we need L = 134 which would then have to be increased to the next power of 2, or 256, to take advantage of the radix-2 FFT algorithm. Assuming the standard cost of a length-L FFT is $\frac{L}{2}\log_2 L$, we find that almost a 13 fold increase in the computational complexity is incurred. Although more efficient FFT implementations exist, where FFT pruning as in [7] and [8] and algorithm optimization techniques can be employed to reduce the complexity, the computational load remains a serious problem for the achievable performance. To illustrate this, the execution time of the ZP(L) estimators for N= 32 and $32 \le L \le 4096$ (with L a power of 2) was measured using the *timeit.m* function in MATLAB [9]. The resulting ratio of the execution times with respect to the length N FFT was found to be {1, 1.27, 1.4, 1.95, 5.4, 7.78, 24.83, and 48.31}. Note that these results are significantly better than the standard radix-2 FFT cost which for a length-1024 FFT would have been 64 times the length-32 FFT as opposed to the factor of 7.78 achieved in MATLAB. Despite this, however, it remains clear that the required increase in L to approach the CRLB can quickly become computationally prohibitive in many applications (especially real-time scenarios.)

Optimized search strategies, such as the dichotomous search for the periodogram peak, originally proposed by Zakharov et al. and then improved in [10], can be used to reduce the computational load.

Optimized search strategies, such as the dichotomous search for the periodogram peak, originally proposed by Zakharov et. al. and then improved in [10], can be used to reduce the computational load. Instead of the direct oversampling of $I(\lambda)$, the dichotomous search algorithm implements a binary search for the peak as depicted in the inset in Fig. 1. Starting with the indices m of the maximum bin, and a step size of Δ, the bins on either side of m are compared and the location of the true maximum narrowed down to the range between m and the second highest bin, in this case the range $[m-\Delta, m]$. The step size is halved and a new bin is calculated in the middle of this interval, i.e., at $m - \Delta/2$, and the procedure repeated to give the new maximum at $m - \Delta/4$. We can see that repeatedly iterating these steps would successively lead us closer to the true maximum. Furthermore, due to the continuous halving of the step size, the resolution of the algorithm after Q iterations is $1/2^Q$. Note that the modified algorithm of [10] uses two overlapping bins originally to stabilize the performance of the search in the absence of zero-padding.

Interpolation on DFT Coefficients

Despite the simplicity of the ZP(L) algorithm and its derivatives such as the dichotomous search, they suffer from a limited resolution that can only be improved with increasing SNR at the expense of increasing computational cost. This limitation may be overcome by using interpolation to locate the true maximum of $I(\lambda)$ and refine the coarse estimate of the MBS. Such a two-stage estimation strategy has been extensively explored in the literature [3], [4], [6], [11]. The interpolation step, or fine estimation stage, usually employs a small number of coefficients (2 to 5) centred on the maximum bin. In [6], an estimator was proposed in which the coarse estimate of the MBS is used to initialize a Newton search for the maximum of $I(\lambda)$. However, [11] shows that the Newton search suffers from convergence problems. Quinn and Macleod developed a number of interpolation-based algorithms that are stable and have good performance (see [4] and [11]). These interpolators have estimation variances that are of the same order as the CRLB but nonetheless still exhibit frequency-dependent performance.

The development in [4] of interpolators that are amenable to iterative implementation allowed uniform performance independent of the true signal frequency to be achieved and led to an improvement in the estimation accuracy. One of these algorithms comprises the following steps (for a MATLAB implementation of this algorithm and other estimators refer to [12]):

- Initialization:
  Let X = FFT(x),
  and $Y[n] = |X[n]|^2, n = 0...N-1$
- Coarse Estimate:
  $m = \arg\max_n \{Y[n]\}$
- Iteration 1:
  $$X_p = \sum_{k=0}^{N-1} x[k] e^{-j2\pi k\frac{m+p}{N}}, \text{ for } p = \pm 0.5$$
  $$\hat{\delta} = \frac{1}{2}\Re\left\{\frac{X_{0.5}+X_{-0.5}}{X_{0.5}-X_{-0.5}}\right\}$$
- Iteration 2:
  $$X_p = \sum_{k=0}^{N-1} x[k] e^{-j2\pi k\frac{m+p+\hat{\delta}}{N}}, \text{ for } p = \pm 0.5$$
  $$\hat{\delta} = \hat{\delta} + \frac{1}{2}\Re\left\{\frac{X_{0.5}+X_{-0.5}}{X_{0.5}-X_{-0.5}}\right\}$$
- Final frequency estimate:
  $$\hat{f} = \frac{m+\hat{\delta}}{N} f_s.$$

The MBS algorithm comprises the first three steps and returns the coarse estimate given by the index m of the maximum bin. Two new coefficients $X_p \equiv X[m+p]$ that are on the edges of the maximum bin, that is for $p = \pm 0.5$, are employed

to interpolate for the location of the maximum. Now for $|\delta| \le 0.5$, the fact that $\frac{2\pi\delta}{N} << 1$ permits the use of the approximation $e^{j2\pi\frac{\delta}{N}} \approx 1 + j2\pi\frac{\delta}{N}$ and gives a fine estimate $\hat{\delta}$ of the residual δ as

$$\hat{\delta} \approx h(\delta) = \frac{1}{2}\frac{X_{0.5} + X_{-0.5}}{X_{0.5} - X_{-0.5}}. \tag{11}$$

Since δ is real-valued, we take the real part of the interpolation function, $h(\delta)$. A second algorithm in [4] differs from that presented above only in its interpolation function which employs the magnitudes of the bins X_p. The approximations employed in arriving at equation (11) produce a bias of order N^{-2}. This bias is lower than the CRLB and can usually be ignored. It only becomes significant for very large SNRs, in which case, an exact formulation in [3] that eliminates it can be employed with the fine estimate

$$\hat{\delta} = \frac{N}{2\pi}\angle\hat{z}$$

$$\text{where } \hat{z} = \frac{1}{\cos\left(\frac{\pi}{N}\right) - 2jh(\delta)\sin\left(\frac{\pi}{N}\right)} \tag{12}$$

and $\angle\hat{z}$ is the angle of $\hat{z}$.

The red curve in Fig. 4 shows the performance of the algorithm after iteration 1. While the ratio of the variance to the CRLB is still frequency dependent with a maximum value of $\pi^2/9 \approx 3.3$, its minimum of $\pi^4/96 \approx 1.1047$ occurs at $\delta = 0$ which is a fixed point of $h(\delta)$ (the fixed point being defined as the value of δ such that $h(\delta) = \delta$). Reference [4] shows that the interpolation function is a contractive mapping; this guaranties that the iterations of the fine search converge to $\delta = 0$, thus ensuring that the estimation variance also converges to its minimum value. We also point out that the iterative implementation eliminates the bias as $h(\delta)$ is unbiased at the fixed point. The green curve in Fig. 4 demonstrates these performance characteristics. Finally, the performance of the algorithm for $N = 32$ is shown as a function of SNR in Fig. 5. The curves for the ZP(L) estimator, for $L = 32$ and 1024, are included for comparison (the MBS and ZP(32) are in fact the same estimator). Observe the difference in performance of the iterative estimator between the first and second iterations. Beside the lower variance, the second iteration eliminates the performance floor that is visible after the first iteration due to the estimation bias.

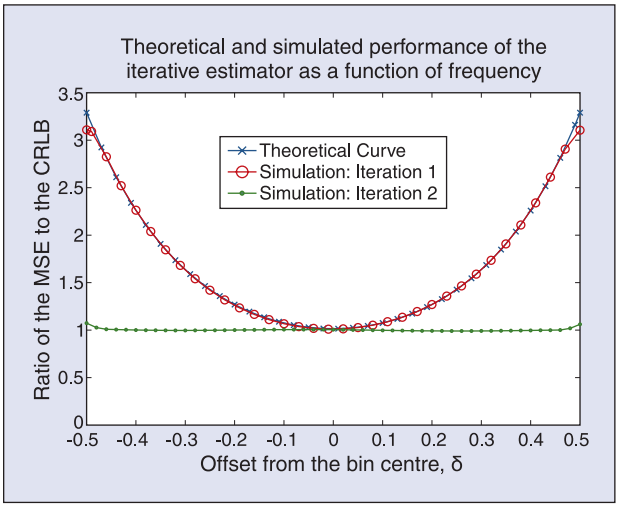

Fig. 4. Performance of the iterative algorithm as a function of frequency.

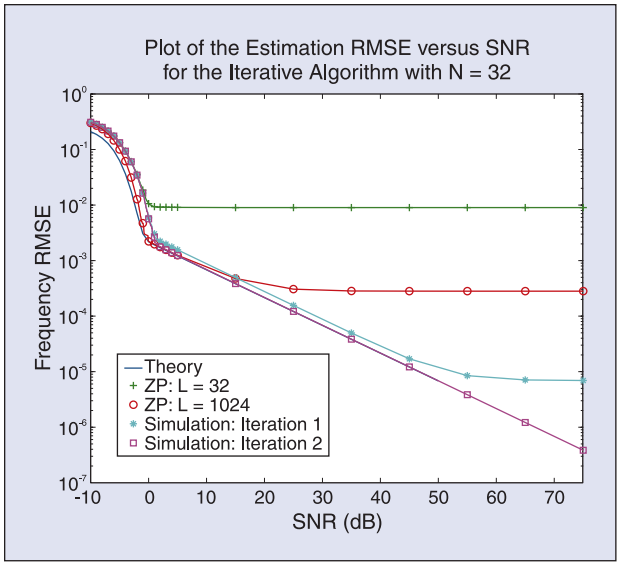

Fig. 5. Performance of the iterative algorithm as a function of signal to noise ratio.

Frequency and Decay Factor of a Decaying Complex Exponential

We now turn our attention to the problem of estimating both the frequency and damping factor of a decaying sinusoid. The CRLB for the damped case, shown in [3], is given by

$$\sigma_\eta^2 = 4\pi^2\sigma_f^2 = \frac{\left(1-e^{-2\eta}\right)^3\left(1-e^{-2N\eta}\right)}{2\rho_0\left[-N^2e^{-2N\eta}\left(1-e^{-2\eta}\right)^2 + e^{-2\eta}\left(1-e^{-2N\eta}\right)^2\right]} \tag{13}$$

where, due to the fact that the signal is decaying, we define the nominal signal to noise ratio $\rho_0 = |A|^2/\sigma^2$. It is interesting to observe that the CRLBs of the decay factor and frequency are scaled versions of one another. In fact, looking at equation (1), we expect that the real and imaginary parts of $\beta = -\eta + j2\pi f$ would be influenced similarly by the noise, giving the same CRLB. The factor 2π leads to increased sensitivity of the observations to changes in the frequency and, hence, to a lower CRLB than that of the decay factor.

The problem of estimating η and f for a single complex exponential in noise was studied in [3]. The estimators of [4] were extended to give an estimate of the decay factor in addition to the frequency and were shown to have excellent

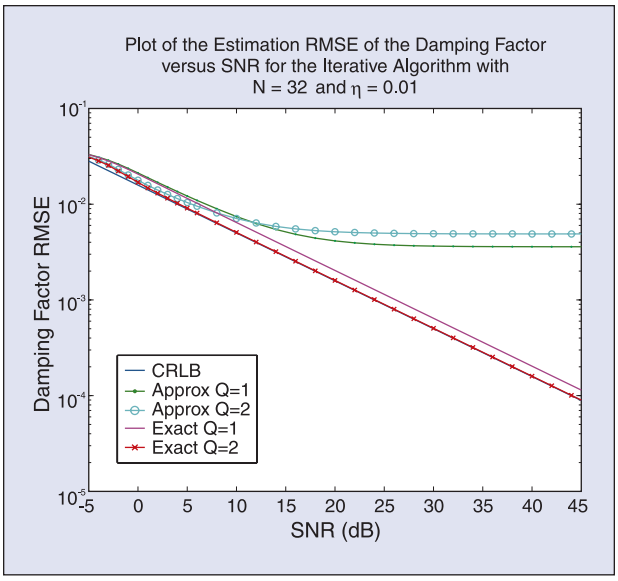

Fig. 6. Performance of the estimator of the damping factor as a function of signal to noise ratio.

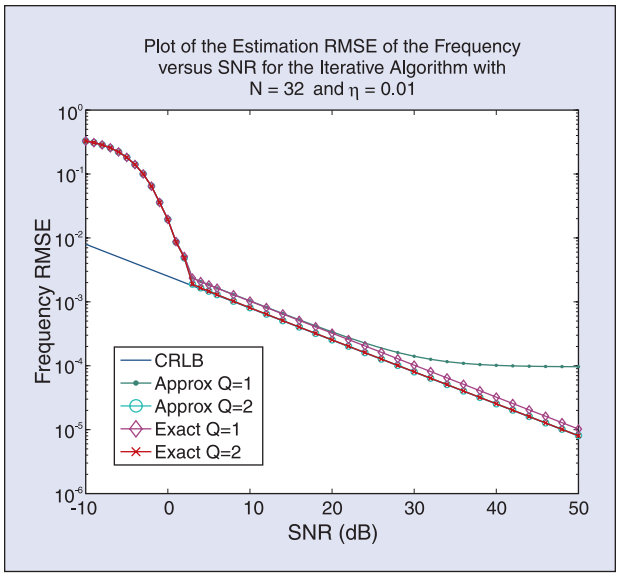

Fig. 7. Performance of the estimator of the frequency as a function of the signal to noise ratio.

performance. The similarity between the two parameters demonstrated by their CRLBs is also reflected in the extension of the iterative estimator to the damped case, yielding the estimates

$$\hat{\eta} \approx \frac{2\pi}{N}\Im\{h(\delta)\}, \text{ and } \hat{\delta} \approx \Re\{h(\delta)\}. \tag{14}$$

As in the un-damped case, the approximations result in estimation biases. Here, however, the presence of the decay factor makes the biases significant when the product $N\eta$ is large enough (that is when the data record is long compared to the decay rate of the signal.) In this case, one should use the exact formulation of the estimator yielding the estimates,

$$\hat{\eta} = -\ln|\hat{z}|, \text{ and } \hat{\delta} = \frac{N}{2\pi}\angle\hat{z} \tag{15}$$

with $\hat{z}$ obtained using (12).

Although the estimator of the frequency is identical to that of the un-damped case, the presence of the decay factor leads to some fundamental differences in the estimation performance. In fact, in the un-damped case, the signal power is $O(N^2)$, whereas the noise terms are $O(N\ln N)$. Thus, the signal terms increase faster than the noise terms with increasing N which permits the asymptotic performance of the algorithms to be established and leads to the estimation variance tracking the CRLB. In the damped case, on the other hand, the signal attenuates with time, and taking a longer data record gives a diminishing rate of return as the CRLB itself asymptotes to a lower limit [3]. Therefore, a sample size N exists beyond which no appreciable improvement in performance can be achieved.

When one considers practical estimators such as those of [3], this effect is more pronounced with the performance initially improving as N is increased, reaching a minimum and then deteriorating. The optimal number of samples is dependent on the decay rate and was found to be $N_{opt} \approx 3/\eta$. The estimation variance and its ratio to the CRLB were also derived in [3] and are functions of the decay factor. Fig. 6 and Fig. 7 show the performance of the algorithms versus the SNR for $N = 32$ and $\eta = 0.01$. A number of samples smaller than the optimum was employed to illustrate the bias effects. First, notice the failure of the approximated estimator of η for the combination of N and η employed here. Even after the second iteration, the performance is still quite poor and in fact does not improve if the estimator is run for additional iterations. This is due to the approximation bias and is in contrast to the estimator of f that still behaves similarly to the un-damped case. The exact expressions, on the other hand, exhibit excellent performance for both η and f.

Conclusion

In this article, we have reviewed the estimation of the frequency of a complex exponential in noise. We examined both the un-damped and damped cases and presented robust, accurate, and computationally efficient estimators for the frequency of the former and the frequency and damping factor of the latter. Although these estimators perform very well on a single exponential, significant challenges remain, and the problem continues to receive significant attention in the literature. (For additional references as well as MATLAB implementations of various estimators, the interested reader may refer to [12].) Two important problems are the multicomponent and the real sinusoid cases. The excellent performance of the estimators presented here extends to the multi-component case only when the components are well separated in frequency. Closely separated components, on the other hand, interfere with one another and produce estimation biases.

The estimation of the frequency of a real sinusoid presents similar issues [1]. A real sinusoid can be expressed as the superposition of two complex exponentials with positive and

negative frequencies, and these act like two components that interfere with one another resulting in estimation biases. In this case, one might be tempted to use the Hilbert transform to obtain an analytic signal before applying estimators designed for complex exponentials. However, care must be taken since discrete implementations of the Hilbert transform (for instance in MATLAB) do not produce a true analytic signal. In such situations, the performance of the estimators on real sinusoids can be quite poor for short data records and frequencies near 0 or ±0.5.

References

[1] T. Radil P. Ramos, and A. Serra, "New spectrum leakage correction algorithm for frequency estimation of power system signals," *IEEE Trans. Instrum. Meas.*, vol. 58, pp. 1670 -1679, May 2009.

[2] T. Lobos, and J. Rezmer, "Real-time determination of power system frequency," *IEEE Trans. Instrum. Meas.*, vol. 46, pp. 877-881, Aug. 1997.

[3] E. Aboutanios, "Estimation of the frequency and decay factor of a decaying exponential in noise," *IEEE Trans. Sig. Process.*, vol. 58, pp. 501- 509, Feb. 2010.

[4] E. Aboutanios and B. Mulgrew, "Iterative frequency estimation by interpolation on Fourier coefficients," *IEEE Trans. Sig. Process.*, vol. 53, pp. 1237-1242, Apr. 2005.

[5] V. Djurović and V. Lukin, "Estimation of single-tone signal parameters by using the L-DFT," *Signal Processing*, vol. 87, no. 6, pp. 1537-1544, Jun. 2007.

[6] D. Rife and R. Boorstyn, "Single tone parameter estimation from discrete-time observations," *IEEE Trans. Inf. Theo.*, vol. 20, pp. 591-598, Sep. 1974.

[7] J. Markel, "FFT pruning," *IEEE Trans. Audio and Electroacoust.*, vol. 19, pp. 305-311, Dec. 1971.

[8] M. Medina-Melendrez, M. Arias-Estrada, and A. Castro, "Input and/or output pruning of composite length FFTs using a DIF-DIT transform decomposition," *IEEE Trans. Sig. Proc.*, vol. 57, pp. 4124-4128, Oct. 2009.

[9] S. Eddins, "The TIMEIT function", MATLAB Central, 2010 [Online]. Available: http://www.mathworks.com/matlabcentral/fileexchange/18798.

[10] E. Aboutanios, "A modified dichotomous search frequency estimator," *IEEE Sig. Process. Lett.*, vol. 11, pp. 186-188, Feb. 2004.

[11] B. G. Quinn and E. J. Hannan, *The Estimation and Tracking of Frequency*, New York: Cambridge University Press, 2001.

[12] The Signal Processing Software Repository, [Online]. Available: http://www.ee.unsw.edu.au/SoftRep/.

Elias Aboutanios (elias@ieee.org) received the Bachelors in Engineering in 1997 from the University of New South Wales (UNSW) and the PhD degree in 2003 from the University of Technology, Sydney (UTS), Australia. In 1993, he was awarded the UNSW Co-op Scholarship, and the following year he was the recipient of the Sydney Electricity Scholarship. In 1997, he joined Energy Australia as an electrical engineer. In 1998, he was awarded the Australian Postgraduate Scholarship and commenced his work toward the PhD degree at UTS. While at UTS, he was a member of the Cooperative Research Center for Satellite Systems team working on the Ka Band Earth station. Between October 2003 and February 2007, he was a research fellow with the Institute for Digital Communications at the University of Edinburgh where he conducted research on Space Time Adaptive Processing for radar target detection. He is currently a senior lecturer at the University of New South Wales. His research interests include parameter estimation, algorithm optimization and analysis, adaptive and statistical signal processing and their application in the contexts of radar, nuclear magnetic resonance, and communications. He is the joint holder of a patent on frequency estimation.

Tutorial Video Clips on IMS Website

Shreekanth Mandayam, Chair, IMS AdHoc Education Committee

The I&M Society's website, http://www.ieee-ims.org, is now hosting short, <20min, tutorial video clips for:

- Undergraduate students and faculty;
- Graduate students and faculty;
- Practitioners in IMS-related areas;
- Practitioners/hobbyists in non-IMS-related areas.

Some of the proposed topics of the video clips include:

- Fundamentals of instrumentation technology and measurement science
- Systems of units and standards
- Signal conditioning and data acquisition
- Laboratory instrumentation basics
- Characterizing a 2-, 3-, 4-port device.
- Ground loop – introduction to EMC
- IEEE 1451 Basics

A distinguished cadre of experts from academia, industry and graduate schools will present these tutorials. In addition to the actual video-clip, the web portal will feature –

- The presence of affinity links to related topics and categories to maximize the availability of existing and future IMS content;
- Social networking links (e.g. e-mail this, blog this) to provide links to the IMS community.

The video clips will be available for a nominal fee for IMS members; will be competitively priced for others; and free to student members.

If you are interested in participating in this exciting project, please e-mail Shreekanth Mandayam at shreek@ieee.og.